

# Multispectral-Polarimetric Sensing for Detection of Difficult Targets.

W A Hubbard, F T Gowen, G J Bishop  
BAE SYSTEMS Advanced Technology Centre  
Filton, Bristol, BS34 7QW

G Innes, D J Jordan, D Hayter, J Ellis  
QinetiQ  
Malvern, Worcestershire WR14 3LG

## Abstract

*The benefits for the detection of difficult targets have been demonstrated for multispectral and polarimetric imagery in differing conditions. The spectral differences between target and background have been seen to provide an enhancement to target discrimination. However, false alarms can occur mainly due to spectral variations in background materials. Complimentarily, polarimetric imagery has been used to detect man made targets by exploiting the reflective characteristics of man-made objects and the suppression of background clutter; but polarimetric imagery for a detection process can be limited by the geometry and nature of targets. The intention of this work has been to investigate whether adding the polarimetric to the multispectral information decreases background induced false alarms whilst maintaining good detection statistics for low contrast targets. This is the second year of the project which has focused on building a data gathering SWIR sensor, data gathering and processing.*

Keywords: Multispectral, Polarimetric, Detection of Difficult Targets, SWIR

## Introduction

Studies have shown that in differing conditions multispectral [1] and polarimetric [2] sensors can enhance target detectability. It has been demonstrated that multispectral imagery can be used to detect low contrast targets using intrinsic spectral differences between target and background. However, multispectral imagery can produce false alarms mainly caused by spectral variations in background materials. Polarimetric imagery has been used to detect man made targets by exploiting the surface finish of these objects compared to the background. However, the performance of polarimetric imagery in isolation can be limited by the geometry and nature of targets. By adding the polarimetric information to the multispectral it may be possible to decrease background induced

false alarms whilst providing good detection statistics for low contrast targets. To evaluate the benefits of combining spectral and polarimetric information, a multispectral-polarimetric sensor operating in the SWIR waveband was constructed. Supporting modelling was also undertaken. The SWIR waveband was selected because commercially available cameras exist. Moreover, it has been observed that a SWIR hyperspectral sensor is particularly effective at defeating targets employing Camouflage Concealment and Deception (CC&D) techniques, as these are conventionally aimed at visual wavelengths. These sensors have also been shown to detect land mines. The SWIR multispectral-polarimetric sensor has been constructed, based around an Indium Gallium Arsenide camera operating in the 1



– 1.7 micron waveband, which operates with a filter wheel to provide spectral information at seven wavebands with 100nm bandwidths. A polariser provides s and p-polarisation data at each waveband, and linear polarisation image cubes are formed for the Stoke's parameters  $S_0$  and  $S_1$ . Polarisation and spectral signatures have been measured from a small number of static targets at short range in the SWIR waveband. Key findings of this work are that the measured polarisation signatures of a painted panel at various orientations are in broad agreement with those predicted by polarimetric theory.

Modelling has been performed to assess waveband selection. The radiance values for all modelling, at each waveband and for each polarisation, were collected by running suitable scenarios through the BAE SYSTEMS SIRUS infrared predictive tool. It incorporates surface optical properties including spectrally-dependent or complex BDRF 'paints', and atmospheric / environmental contributions by including an embedded version of the standard MODTRAN code. Surface temperature is imported as part of the surface model geometry. SIRUS has been used extensively by BAE SYSTEMS Air Systems, Warton for L.O. Studies, and validated against M.o.D supported engine, plume and surface optics trials and studies (RAPS, Mohican and SOAR).

### **SWIR Modelling**

The modelling has been undertaken for the waveband 1.0  $\mu\text{m}$  to 1.6  $\mu\text{m}$ , with seven 0.1  $\mu\text{m}$  sub-bands for the multispectral-polarimetric analysis [3].

Material descriptions were extracted parameters from measured HDR polarimetric data fitted to a cosine polynomial model of the reflectances, and hence apparent radiance values determined. The data was fitted to a model of purely specular reflection. Modelling was limited by the material properties data currently available. Discrimination for the case of

painted panel material against a tarmac background has been assessed.

The contrast between target objects and background were reduced to provide difficult cases for the detection processing. All modelling performance assessments were completed with a 1976 US Standard atmosphere, as defined in Modtran.

Image multispectral cubes were constructed of background with variability applied and flat green-painted targets embedded for each of the s-polarisation and p-polarisation data, and thereafter for each of the Stokes parameters  $S_0$  and  $S_1$ .  $S_0$  is the total intensity, given by the sum of the intensities measured using two orthogonal linear polariser orientations.  $S_1$  is the difference in intensities, and is zero for unpolarised radiation. Variability in the background was applied by assuming a Gaussian distribution. Single pixel targets were embedded in a background at each of the sub-bands. The image multispectral cubes were converted to apply to a standard multispectral imager, and subsequently had a generic sensor noise term added [3]. The final image multispectral cubes were passed through a multispectral anomaly detection algorithm [4], and detection statistics in the form of Receiver Operator Characteristics (ROC) curves collected.

It was found that four wavebands together with polarimetric information gave best detection performance. These wavebands correspond to higher values in the covariance matrix generated from the simulated imagery, and also align with high values or gradients in atmospheric transmission in the SWIR region, at 1.0, 1.2, 1.5 and 1.6  $\mu\text{m}$ .

### **SWIR Sensor Build**

The sensor used is based on a 320x240 pixel Sensors Unlimited 12 bit digital InGaAs camera operating between 1 $\mu\text{m}$  and 1.7 $\mu\text{m}$ . The camera lens is a 7.6° field of view conventional glass camera lens. A polariser fitted into a hand-operated rotation

stage is used as the analyser. Multispectral operation in the SWIR waveband has been provided by a motorised rotating wheel into which seven SWIR filters can be inserted, one aperture has been left open for broadband operation (Figure 1).

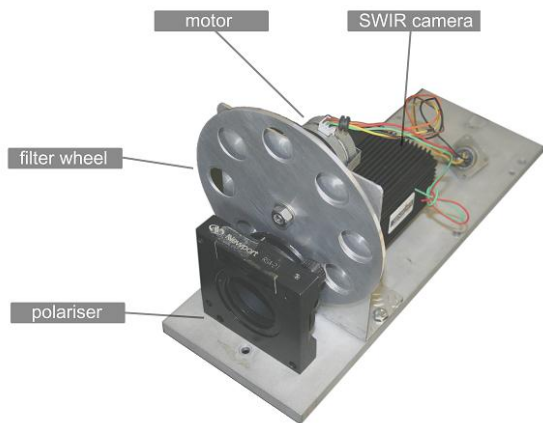


**Figure 1 - SWIR Multispectral - Polarimetric Sensor**

Spectral filters have been procured to span the 1.0-1.7 $\mu$ m waveband. It was necessary to identify suppliers of filters with the correct performance that are also suitable for use in an imaging system. Some commercially available filters are fabricated on thin substrates and these can distort during manufacture. Imaging is not always a prime application for these filters and small distortions are not an issue. However, for this task, it is crucial that the distortions are very small. The SWIR filters used in the sensor are 100nm FWHM bandpass filters with centre wavelengths at 1000, 1100, 1200, 1300, 1400, 1500, and 1600 nm supplied by Omega Optical, Inc..

The scale of this project has not permitted the construction of a sensor that could acquire the polarisation sub-images simultaneously. All components in the sensor are attached to a metal base plate, mounted on a tripod. The integration time of the camera is controlled through a hyperterminal. Any additional compensation for light levels is addressed through the use of neutral density filters. In operation the polariser was rotated through

0° and 90°, and at each step one image was acquired. Manipulations of the resulting images permitted the relevant Stokes parameters to be determined for each pixel. Registration of the components of the image cubes is key to best performance with any subsequent detection processing, as any misalignment will cause spurious artefacts. It took approximately 2 minutes to acquire each image.

### Joint SWIR Multispectral - Polarimetric Sensor and Hyperspectral Sensor Trials

Data was gathered at regular intervals over a number of days and two locations, in tandem with a hyperspectral imager. A typical target scene is shown in RGB (Figure 2), with all objects shown. A second location was also used to collect scene data without the influence of nearby foliage. A panel was mounted at elevations to provide approximately 60° and 30° angles of incidence to the line of sight of the sensors and 0° azimuth for the trials.

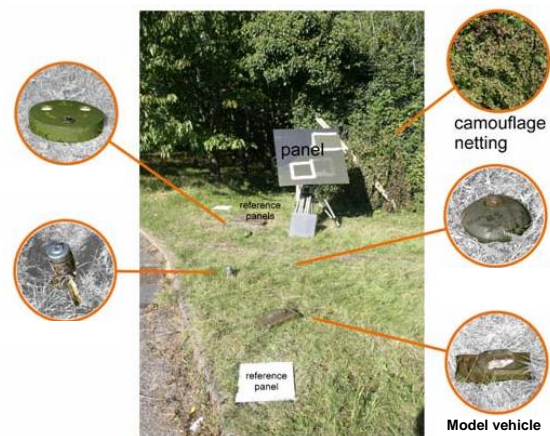


**Figure 2 – RGB Image of a Scene and Objects**

Atmospheric transmission in this waveband is dominated by water absorption bands at 1.14 and 1.4  $\mu$ m wavelengths. Normalised spectra as measured with the ATC Hyperspectral sensor show that similar materials give similar vectors (Figure 3). Here it shows that relatively lower values in radiance are found at the longer

wavelengths in pixels containing vegetation, due to a lower reflectance. In this case, similar behaviour at the panel pixels could be due to illumination reflected from the surrounding vegetation, reducing the irradiance at these wavelengths.

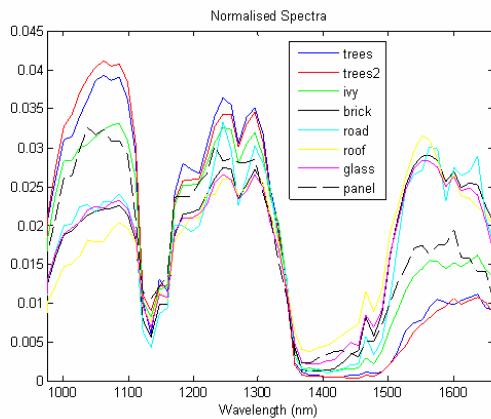


**Figure 3 –  $S_0$  Spectra at the Sensor**

Example images of  $S_0$  and  $S_1$  Stoke's parameter images at 1.0  $\mu\text{m}$  are given in Figure 4 and Figure 5 respectively. It can be seen that background clutter is reduced in the  $S_1$  image.



**Figure 4 –  $S_0$  Image at 1.0  $\mu\text{m}$**

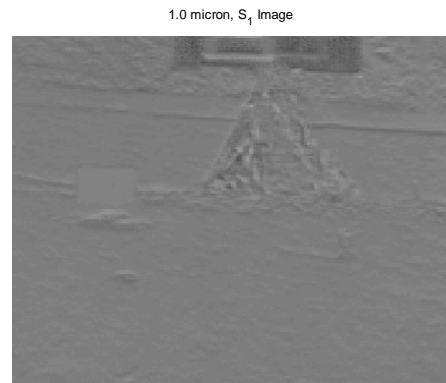


**Figure 5 –  $S_1$  Image at 1.0  $\mu\text{m}$**

This point is further demonstrated by samples of pixel spectra taken with the SWIR Multispectral-polarimetric sensor of two material types, and for  $S_0$  and polarimetric  $S_1$  images. The relative 'significance' of the panel spectra with respect to the grass spectra is improved in the  $S_1$  images, which suggests the possibility of higher detection performance due to background suppression (Figure 6).

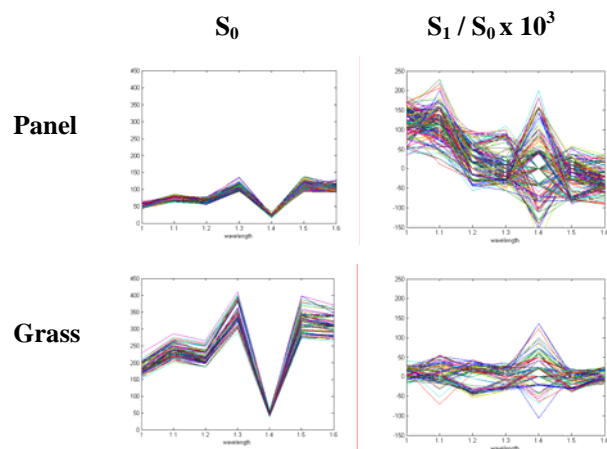


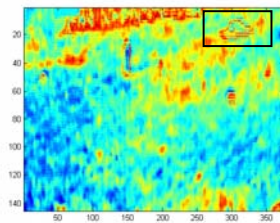
**Figure 6 –  $S_0$  and  $S_1$  Spectra**

The data show that low s-polarisation and p-polarisation values at 1.4  $\mu\text{m}$  give rise to noisy values in  $S_1$  at this waveband, and polarimetric signature appears to be negligible at the higher wavelengths 1.5 and 1.6  $\mu\text{m}$ .

## Registration of SWIR Multispectral-Polarimetric data

Currently the SWIR Multispectral-Polarimetric sensor outputs the polarisation data at each waveband separately, and the image cubes for detection processing are registered and built off-line. Correct registration of the components is a significant issue which can degrade performance results if not undertaken with sufficient care. An image set has been analysed, firstly registered by comparing the position of an object in the scene, subsequently single pixel shifts were applied, and a difference image inspected for quality to provide a re-registered image cube. An example of the effects on the detection process can be demonstrated by applying a Spectral Angle Mapping (SAM) matched filter to the initial registered image cube, and also to the re-registered image cube. Identification of the structure of a model vehicle demonstrates that detection is superior when the image cube registration is improved (Figure 7).

### First Pass Registration



### Improved Registration

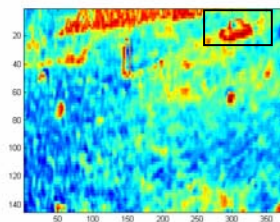


**Figure 7 - Effects of Single Pixel Re-registration on Detection Results**

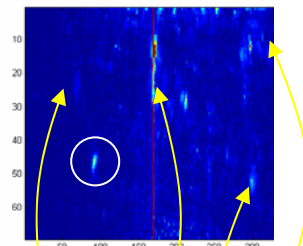
### Analysis of Joint Trials Data

Spectral analysis with a SAM filter was investigated. This technique gave best results for unpolarised image data, which

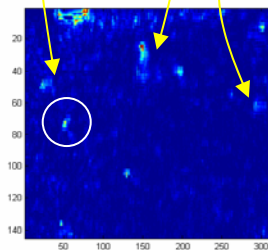
can be understood as just two of the wavebands adopted show appreciable spectral information in the  $S_1$  images (at 1.0 and 1.1  $\mu\text{m}$ ), and values are dependant on the incidence angles to the materials. A fusion of post-detection spectral and polarimetric analysis may prove to be complimentary.

Global RX Detection was performed on corresponding images (Figure 8). The number of bands was reduced to eight in the hyperspectral image to facilitate processing for this analysis, at the centre of each of the Multispectral-Polarimetric filter wavebands plus at 1650 nm. The result from processing the hyperspectral sub-image has high values in a column of the image, this effect is seen where there is a discontinuity of intensity in the original image or a saturation of a pixel. It is believed to be an artefact of the sensor affecting the statistics of image pixels below that point, which although not visible affects RX output.

### Hyperspectral



### Multispectral-Polarimetric, $S_0$



### Multispectral-Polarimetric, $S_1$

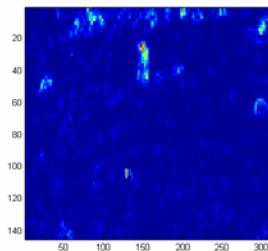


**Figure 8 - Global RX Anomaly Detection Results**

Pixels on objects can be identified in the hyperspectral and the multispectral-polarimetric  $S_0$  images (corresponding objects are identified with yellow arrows in the figure), also pixels on a similar sized stone (circled in the figure), however there are other high values which may give rise to false alarms. The multispectral-polarimetric  $S_1$  image finds more pixels on the targets, and suffer less with high values in the background, also it can be seen that different parts of target objects are found, which would be expected to correspond to surfaces at preferential incidence angles. Although not shown here, processing the  $S_1$  broadband image cube was not as successful at detecting the objects, locating just two of the four objects.

A change detection algorithm which operates spectrally has been developed. The whole image result is shown together with a sub image in Figure 9.

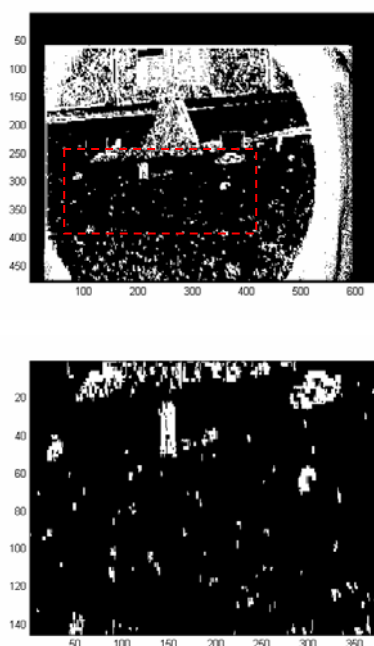


**Figure 9 - Spectral Change Detection Analysis**

The algorithm identifies polarised objects in the multispectral-polarimetric data by looking for changes between s-polarisation

and p-polarisation spectral values. With a threshold applied to the results to give a monochrome result, the target objects are clear and the structures identifiable.

## Conclusions

Spectral processing has been undertaken on objects of interest in complicated scenes, and against natural materials. It is believed that spectral characteristics have been affected by surrounding materials, notably by overhanging foliage which may reduce illumination around the 1.5 to 1.6  $\mu\text{m}$  wavelengths.

Matched filtering performance on intensity images is improved with the greater number of wavebands used in the hyperspectral data processed. Processing on the  $S_1$  images is sensitive to the angle of incidence of surfaces of polarimetric materials, which together with object identification could be used to give additional information about structure within the object as an additional aid to target detection, or to reduce false alarms.

RX anomaly detection has shown better results when processing the  $S_1$  spectral data, compared to  $S_0$  spectral data and also corresponding  $S_1$  broadband images.

A change detection algorithm which works spectrally has produced promising results when used to compare the two polarisation states, and has clearly identified objects of interest in a scene.

It is believed that results support the view that a suite of algorithms, able to compare and contrast results from individual processes, could be developed for the SWIR Multispectral-Polarimetric sensor which by offering complimentary information could improve detection performance.

## References

- 1 G.Bishop and A.Killey "Final Report on RCSC18 Sensor Technologies for Future

- Tactical UAVs Research Study”.  
TES100935 Sept. 2006
- 2 D Jordan, G Innes and D Hayter  
“Polarimetric Imaging”. Journal of  
Defence Science, Vol. 10, No. 3, R166-  
172 (2005)
  - 3 Eismann et al. “Comparison of Infrared  
Imaging Multispectral Sensors for  
Military Target Detection Applications”.  
SPIE Vol. 2819 / 95.
  - 4 I.S.Reed and X.Yu “Adaptive Multi-  
band CFAR Detection of an Optical  
Pattern Unkown Spectral Distribution”.  
IEEE Trans. Acoustics, Speech, Signal  
Processing, Vol. 38, pp.1760-1770, Oct.  
1990

### **Acknowledgements**

The work reported in this paper was funded by the Electro-Magnetic Remote Sensing (EMRS) Defence Technology Centre, established by the UK Ministry of Defence and run by a consortium of SELEX Galileo, Thales UK, Roke Manor Research and Filtronic.